33rd Annual International Conference of the IEEE EMBS
Boston, Massachusetts USA, August 30 - September 3, 2011

Detection of malaria parasites in thick blood films

Matthias Elter, Erik Haßlmeyer and Thorsten Zerfaß
Fraunhofer Institute for Integrated Circuits IIS
Image Processing and Medical Engineering Department
Am Wolfsmantel 33, 91058 Erlangen, Germany
erik.hasslmeyer@iis.fraunhofer.de

Abstract— **Malaria, caused by a blood parasite of the genus plasmodium, kills millions of people each year. According to the World Health Organization, the standard for malaria diagnosis is microscopic examination of a stained blood film. We have developed a two-stage algorithm for the automatic detection of plasmodia in thick blood films. The focus of the first stage is on high detection sensitivity while accepting high numbers of false-positive detections per image. The second stage reduces the number of false-positive detections to an acceptable level while maintaining the detection sensitivity of the first stage. The algorithm can detect plasmodia at a sensitivity of 0.97 with a mean number of 0.8 false-positive detections per image. Our results indicate that the proposed algorithm is suitable for the development of an automated microscope for computer-aided malaria screening.**

I. Introduction

Malaria is an infectious disease, with a high prevalence in tropical and subtropical regions, caused by a blood parasite of the genus plasmodium. It is transmitted by the bite of a female anopheles mosquito. Approximately 243 million cases led to nearly 863.000 deaths in 2008 [1]. Four species of the genus plasmodium can infect humans and cause malaria: plasmodium falciparum, plasmodium vivax, plasmodium ovale, and plasmodium malariae. The most serious forms of malaria are caused by plasmodium falciparum. According to the World Health Organization (WHO), microscopic examinations of stained blood films are the "'gold standard"' for malaria diagnosis [2]. Two kinds of blood films are used for malaria diagnosis: thin and thick. A thick film is always used to search for malaria parasites as it consists of many layers of blood cells and allows examining relatively large amounts of blood. However, often the parasite species (e.g. plasmodium vivax) can not be confirmed based solely on a thick film. Hence, usually a thin film is prepared for the characterization of the species of parasites that have been detected in the thick blood film. According to the WHO, routine examination of thick films is based on the examination of at least 100 microscopic fields of view at high magnification ($100\times$ objective, $10\times$ ocular). This process is tedious and tiring for laboratory assistants and requires special training and substantial expertise. It also seems to be error-prone, as studies have shown that high intra- and inter-observer variabilities exist in the resulting parasite density quantizations [3], [4], [5]. Therefore, computer-aided detection (CADe) systems are required that support the laboratory assistants in the detection and counting of plasmodia in thick blood films. In Figure 5 example plasmodia, cropped from thick blood film images, are displayed.

Several approaches to the computer-aided detection (CADe) of malaria, based on automatic microscopic detection and characterization of plasmodia in blood films have been proposed in the last years. We provide an overview of the most important articles in the following. A broader overview of the state of the art can be found in a recent review article by Tek et al. [6].

Diaz et al. [7] proposed an approach for quantification and classification of erythrocytes infected with plasmodium falciparum. Their approach has a segmentation and a classification stage. In the segmentation stage, erythrocytes are identified and segmented by means of luminance correction, pixel-classification, and an inclusion-tree representation. In the classification stage, infected erythrocytes are identified and different infection stages are characterized.

Le et al. [8] presented a semi-automatic approach for the quantification of erythrocytes infected with plasmodium falciparum in thin blood films. Their approach is based on an analysis of the co-localization of detected erythrocytes and potential plasmodia. Even though their work is based on thin films, which are especially suited for species differentiation, their work does not cover this aspect.

Tek et al. [9] proposed a two-stage approach for detection of plasmodia in thin films. Bayesian pixel-classification is employed to find plasmodia candidates in the first stage. A kNN classifier based on shape, histogram, and statistical moment features is used in a second stage to reduce the number of false-positive detections.

Additional approaches for the detection of plasmodia in thin films have been proposed by Ross et al. [10] and Di Ruberto et al. [11].

Plasmodia detection based on thick films is the recommended standard proposed by the WHO and is approximately ten times more sensitive than based on thin films [2]. Still, only a single article, published recently by Frean [12], covers the automatic detection of plasmodia in thick films. Frean proposes a straight-forward detection approach based on open-access software that is able to estimate medium to high parasite densities with good accuracy, but is not suited for lower plasmodia densities (fewer than six parasites per image).

In this work we present a novel approach to the automatic detection of malaria parasites in thick blood films. Our

978-1-4244-4122-8/11/$26.00 ©2011 IEEE

work focuses on the detection of plasmodium falciparum parasites as this species is responsible for about 80% of all malaria cases and for about 90% of all malaria deaths. Three growth stages of plasmodia can be found in peripheral blood: trophozoites, schizonts, and gametocytes. However, plasmodium falciparum infections are special because schizonts are usually not, and gametocytes are only rarely seen in peripheral blood. Therefore, we focus on the detection of trophozoites. Our approach tackles the problem of accurate detection independent of plasmodia density.

The rest of this paper is organized as follows. We provide descriptions of materials and methods in Sections II and III, followed by experiments and results in Section IV. We close with a discussion in Section V.

II. Materials

We have acquired 256 1000×1000 pixel Giemsa-stained thick blood film images at high magnification using a $100\times$ Zeiss oil immersion objective with an optical aperture of 1.3, attached to a Zeiss Axio Imager microscope, and a color CCD digital camera. Care was taken to ensure consistent lighting conditions and white balance for all images. Figures 2 shows part of a sample image form our data set. We have randomly split this image set into two subsets (128 images each) for training and testing. The training set is used for algorithm development, parameter adjustment, and training of a classifier. The test set is solely used for evaluation of the detection performance.

III. Methods

Our detection algorithm has two stages. The focus of the first stage (plasmodia detection) is on high detection sensitivity, with the drawback of relatively high numbers of false-positive detections. The second stage (false-positive reduction) employs a support vector machine (SVM) classifier to reduce the number of false-positive detections to an acceptable level while maintaining the detection sensitivity of the first stage.

A. Plasmodia detection

In this stage, plasmodia candidates are detected with a focus on high sensitivity while accepting potentially low specificity. This means, the algorithm is designed to miss no, or only very few, plasmodia with the potential drawback of many false-positive detections. As stated in the introduction, the detection focuses on the trophozoite growth stage of plasmodium falciparum parasites. Trophozoites appear as small rings or parts of rings with one ore two chromatin dots. Besides plasmodia, the only blood components that contain chromatin are leukocytes and platelets. Therefore, the first step of our detection algorithm is to find objects containing chromatin. We have identified the proportion of the green and the blue component of a blood film image as a very good feature to identify objects containing chromatin in Giemsa-stained blood films. It is not only a highly discriminative feature but also almost independent of differences in illumination and staining intensity. Let $I_{green}(x, y)$, and $I_{blue}(x, y)$ denote the green and blue channels of the input image. We transform the color input image into a monochrome image $I(x, y)$, that highlight objects containing chromatin, based on Equation 1.

$$I(x, y) = \arctan\left(\frac{I_{green}(x, y)}{I_{blue}(x, y)}\right) \quad (1)$$

In the resulting monochrome image $I(x, y)$ objects with chromatin have dark, and objects that do not contain chromatin have bright gray values. The next step of the algorithm is to separate potential plasmodia from other objects that contain chromatin: leukocytes, platelets, and artifacts (such as splintered parts of leukocytes). Plasmodia can be separated from leukocytes based on their characteristic shape. They can be separated from platelets based both on their characteristic shape and staining intensity. Separating plasmodia from artifacts is more difficult and, therefore, is not tackled in this stage of the algorithm. We found the black-top-hat morphological operator [13] to be an excellent mechanism to separate plasmodia from both leukocytes and platelets. The black-top-hat operator is defined as a morphological closing (dilation followed by erosion) of an image followed by the subtraction of the closed image from the input image. We use the generalization of this morphological operator from binary to monochrome images, and a special non-flat structuring element to achieve a separation of plasmodia from leukocytes and platelets. We have found a non-flat structuring element that represents a paraboloid to be very well suited for this task. The slope of the paraboloid is chosen to be one, and the radius (which is based on the typical size of plasmodia) to be seven pixel. These parameters are fixed for our system and need to be adjusted only in case of a change in pixel size (i.e. when the camera or the objective is changed). Figure 1 illustrates the paraboloid structuring element.

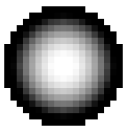

Fig. 1. Illustration of the non-flat structuring element representing a paraboloid. In this case the paraboloid has a radius of nine and a slope of one pixel.

The black-top-hat operator is followed by a threshold operation. Due to the independence of the proportion of the green and the blue component with regard to illumination and staining intensity, we found a global, fixed threshold sufficient for this step. We apply a morphological dilation with a circular, flat structuring element to merge neighboring blobs in the binary image resulting from the threshold operation. The radius of the circular structuring element is chosen to equal the radius of the structuring element used in the black-top-hat operator. The final step of this detection stage is the extraction of plasmodia candidate positions by using a simple connected-components labeling algorithm to extract objects from the binary image. The centroids of

the extracted objects are regarded as plasmodia candidate positions. Figures 2 to 4 illustrate the major steps of the plasmodia candidate detection stage.

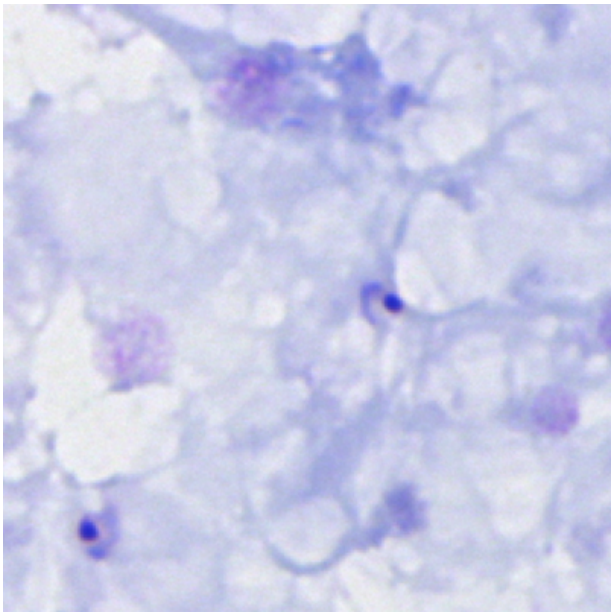

Fig. 2. Part of a sample input image showing two plasmodia.

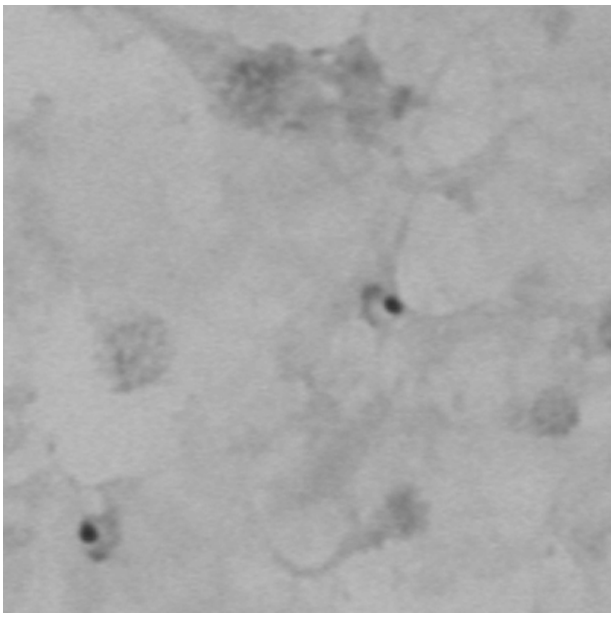

Fig. 3. The input image is converted to a monochrome image that highlights objects containing chromatin.

B. False-positive reduction

Because of the focus on high sensitivity, many plasmodia candidates detected in the previous stage are false-positive detections. Hence, a false-positive reduction step is applied as a second stage of the detection algorithm. The basic idea of this stage is to crop a small region of interest (ROI) for each plasmodia candidate from the input image, to extract a set of features from the ROI, and to classify the ROI based on the feature set as "'plasmodium"' or "'artifact"'. More precisely, we crop ROIs of size 80×80 pixel centered on the plasmodia candidate positions from the input image. We extract a large set of features, including statistical moment features, texture analysis features, and color features. The set of statistical moment features contains four central moments (mean, variance, skewness, and kurtosis), Hu's set of seven invariant moments [14], and the 49 Zernike moments of orders up to 12 [15]. The texture features include Haralick's 13 co-occurance matrix features [16], Unser's 18 sum and difference histogram features [17], Chen's 16 statistical geometrical features [18], and five features proposed by Young et al. [19] that describe the distribution of chromatin in the ROI. The color features include 60 features representing a 60-bin histogram of the hue channel of the ROI, and two features described by Kovalev et al. [20] that represent cyan shifts in the ROI. In total, the feature space has 174 dimensions which requires a selection of a feature subset to avoid the curse of dimensionality. Furthermore, all features are normalized to have zero mean and a standard deviation of one. We select an optimal feature subset in a two-stage process. First, we apply an univariate ranking to keep only the 60 features that have the highest univariate discriminative power. Then we use a genetic algorithm (GA), as suggested by Vafeie and De Jong [21], for automatic selection of an even smaller feature subset. The main issues in applying a GA to a specific problem are to select a reasonable objective function as well as an adequate representation of candidate problem solutions (individuals). An appropriate and simple representation of individuals for the problem of selecting a good subset from a set of N features is a binary string of length N. If the bit at position i, with $0 \leq i \leq N$ is set to one, the ith

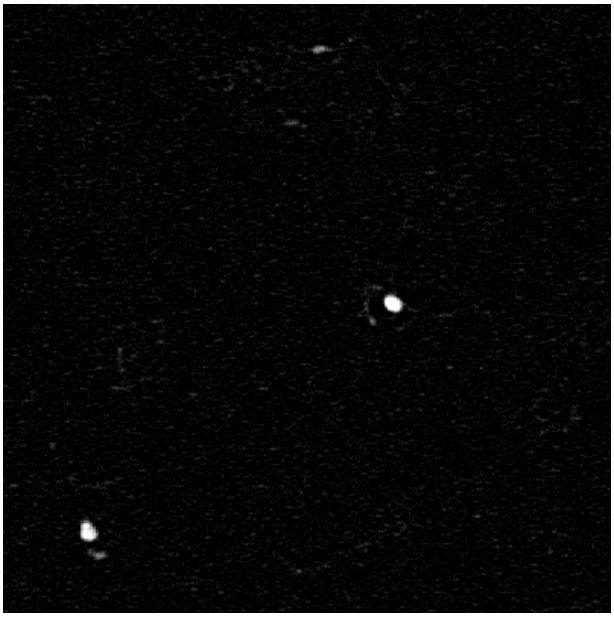

Fig. 4. A black-top-hat operator is applied to the monochrome image to identify plasmodia candidates.

feature is included in the subset represented by the respective individual. As an objective function we use the area under the ROC curve obtained from the classification with the selected feature subset. To avoid a feature selection bias, the selection is based strictly on the training image set and not on the test image set. Once a good feature subset is selected, a SVM is trained based on this feature subset and the training data set to solve the two-class classification problem of classifying a ROI as "'plasmodium"' or "'artifact"'. We use a SVM with a radial basis function kernel with $\gamma = 0.125$, and a cost factor of $C = 1.0$ for this task.

IV. Experiments and results

We have evaluated the performance of our two-stage plasmodia detection algorithm as follows. We extract a set of 266 80×80 pixel ROIs containing all annotated ground-truth plasmodia present in the training data set. Furthermore, we have applied the first stage of the detection algorithm to the training data set to obtain a set of 612 80×80 pixel ROIs showing false-positive detections. The training of the second stage of the detection algorithm is based on these ROI sets. Example ROIs are displayed in Figures 5 and 6.

Fig. 5. Examples of ground-truth plasmodia ROIs.

Fig. 6. Examples of false-positive detection ROIs (resulting from stage one of the detection algorithm).

A feature set is extracted from each ROI, and an optimal feature subset is obtained as described in the previous section. Then the SVM is trained based on the feature subsets of the 266 ground-truth plasmodia and the 612 false-positive detections extracted from the training data set. The evaluation of the detection performance is based on the test data set. The first stage of the detection algorithm is applied to all images of the test set to obtain plasmodia candidate positions. Each plasmodia candidate is represented by a feature vector extracted from a ROI centered on the detected position and classified using the SVM. Plasmodia candidates that are classified as "'artifact"' are considered as false-positive detections and discarded. The remaining candidates are considered as plasmodia. The ground-truth segmentations of the test data set are used to identify each detection as true-positive (TP) or false-positive (FP). The true-positive rate (TPR), also called the sensitivity, and the mean number of false-positive detections per image (FPI) are calculated based on these values. We have obtained pairs of TPR and FPI values by using different values for the threshold parameter of the first detection stage. The TPR and FPI pairs are plotted as a free-response receiver operating characteristic (FROC) curve in Figure 7. To investigate the effects of the false-positive reduction stage, we have also plotted TPR and FPI pairs for the same setup, but with disabled false-positive reduction. At a reasonable sensitivity of 0.97, our algorithm operates at 3.2 FPI without false-positive reduction, and 0.8 FPI with false-positive reduction.

V. Discussion

We have developed a two-stage algorithm for the automatic detection of plasmodia in thick blood films. Our work focused on the detection of plasmodium falciparum parasites as this species is responsible for about 80% of all malaria cases and for about 90% of all malaria deaths. In contrast to the state of the art, our approach tackles the problem of accurate plasmodia detection in case of low plasmodia densities (less than five plasmodia per image). Our results show that high plasmodia detection sensitivity (0.97) combined with low numbers of false-positive detections per image (0.8) can be achieved. This indicates that our approach is suitable for the development of an automated microscope for computer-aided malaria screening. According to WHO guidelines, 100 high magnification fields of a thick blood film must be examined for malaria detection. This tiring and time consuming process could be reduced to a less time consuming examination of the plasmodia candidate detections ROIs returned by our algorithm. There is room for improvements in both stages of our algorithm. We expect that further reductions of the number of false-positive detections are possible and will focus our research on better features for the discrimination of plasmodia and artifacts. A major goal is also the acquisition of larger training and testing data sets for improvements in the robustness of our approach.

References

[1] World Health Organization. *World malaria report 2009*. WHO Press, 2009.

[2] World Health Organization. *Basic malaria microscopy, 2nd edition*. WHO Press, 2010.

[3] Russell E Coleman, Nongnuj Maneechai, Nattawan Rachaphaew, Chalermpol Kumpitak, R. Scott Miller, Virat Soyseng, Krongthong Thimasarn, and Jetsumon Sattabongkot. Comparison of field and expert laboratory microscopy for active surveillance for asymptomatic plasmodium falciparum and plasmodium vivax in western thailand. *Am J Trop Med Hyg*, 67(2):141–144, Aug 2002.

[4] Wendy Prudhomme O'Meara, F. Ellis McKenzie, Alan J Magill, J. Russ Forney, Barnyen Permpanich, Carmen Lucas, Robert A Gasser, and Chansuda Wongsrichanalai. Sources of variability in determining malaria parasite density by microscopy. *Am J Trop Med Hyg*, 73(3):593–598, Sep 2005.

[5] Wendy Prudhomme O'Meara, Mazie Barcus, Chansuda Wongsrichanalai, Sinuon Muth, Jason D Maguire, Robert G Jordan, William R Prescott, and F. Ellis McKenzie. Reader technique as a source of variability in determining malaria parasite density by microscopy. *Malar J*, 5:118, 2006.

[6] F Boray Tek, Andrew Dempster, and Izzet Kale. Computer vision for microscopy diagnosis of malaria. *Malaria Journal*, 8(1):153, 2009.

[7] Gloria Diaz, Fabio A. Gonzalez, and Eduardo Romero. A semi-automatic method for quantification and classification of erythrocytes infected with malaria parasites in microscopic images. *J. of Biomedical Informatics*, 42(2):296–307, 2009.

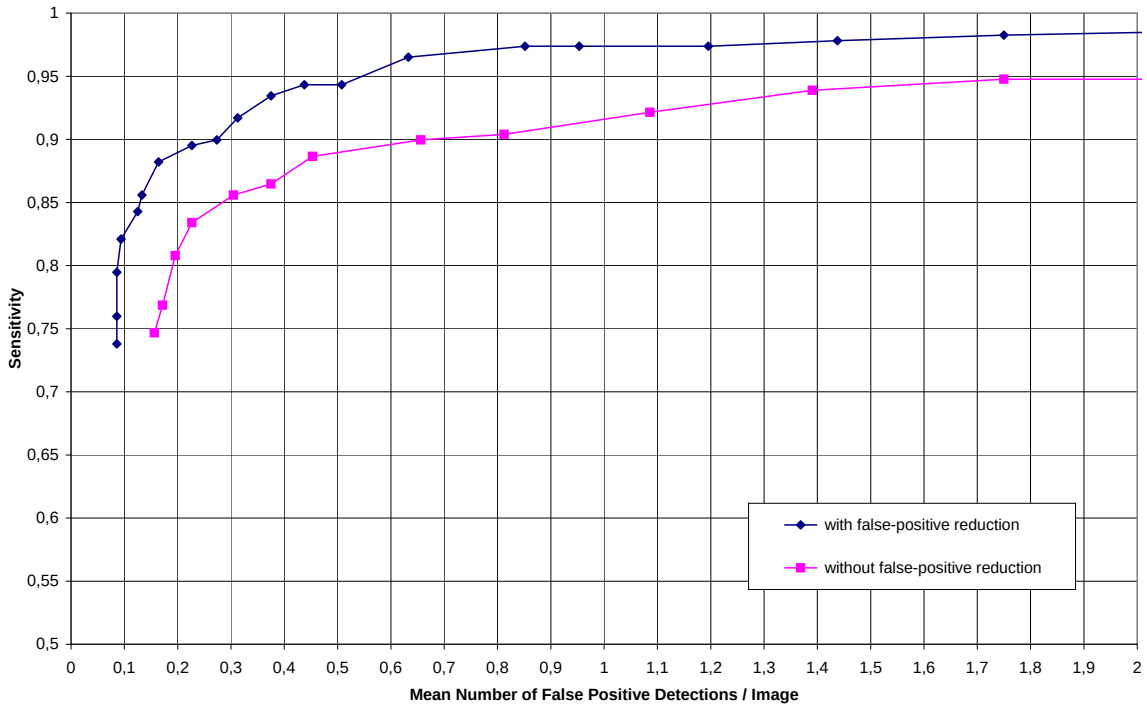

Fig. 7. Sensitivity and false-positive detections per image plotted as a FROC curve (with and without false-positive reduction).

[8] Minh-Tam Le, Timo R Bretschneider, Claudia Kuss, and Peter R Preiser. A novel semi-automatic image processing approach to determine plasmodium falciparum parasitemia in giemsa-stained thin blood smears. *BMC Cell Biol*, 9:15, 2008.

[9] F. Boray Tek, Andrew G. Dempster, and Izzet Kale. Malaria parasite detection in peripheral blood images. In *British Machine Vision Conference 2006 (BMVC2006)*, pages 347–356, 2006.

[10] Nicholas E. Ross, Charles J. Pritchard, David L. Rubin, and Adriano G. Duse. Automated image processing method for the diagnosis and classification of malaria on thin blood smears. *Medical and Biological Engineering and Computing*, 44(5):427–436, 2006.

[11] C. Di Rubeto, A. Dempster, S. Khan, and B. Jarra. Analysis of infected blood cell images using morphological operators. *Image and Vision Computing*, 20(2):133–146, February 2002.

[12] John Frean. Reliable enumeration of malaria parasites in thick blood films using digital image analysis. *Malaria Journal*, 8(1):218, 2009.

[13] J. C. Russ. *The Image Processing Handbook*. IEEE Press, Boca Raton, Florida, USA, 1995.

[14] M.K. Hu. Visual pattern recognition by moment invariants. *IRE Trans. on Information Theory*, IT-8:179–187, 1962.

[15] A. Khotanzad and Y. H. Hongs. Invariant image recognition by zernike moments. *IEEE Transactions on Pattern Analysis and Machine Intelligence*, 12(5):489–497, 1990.

[16] R. M. Haralick, K. Shanmugam, and I. Dinstein. Textural features for image classification. *IEEE Transactions on Systems, Man, and Cybertinetics*, 3(6):610–621, 1973.

[17] M. Unser. Sum and difference histograms for texture classification. *IEEE Trans. Pattern Anal. Mach. Intell.*, 8(1):118–125, 1986.

[18] Y. Q. Chen, M. S. Nixon, and D. W. Thomas. Statistical geometric features for texture classification. *Pattern Recognition*, 28(4):537–552, 1995.

[19] I. T. Young, P. W. Verbeek, and B. H. Mayall. Characterization of chromatin distribution in cell nuclei. *Cytometry*, 7(5):467–474, Sep 1986.

[20] V.A. Kovalev, A. Y. Grigoriev, and H-S. Ahn. Robust recognition of white blood cell images. In *ICPR '96: Proceedings of the International Conference on Pattern Recognition (ICPR '96) Volume IV-Volume 7472*, page 371, Washington, DC, USA, 1996. IEEE Computer Society.

[21] H. Vafaie and K. De Jong. Genetic algorithms as a tool for feature selection in machine learning. In *Proceedings of the 4th International Conference on Tools with Artificial Intelligence*, pages 200–204, Arlington, VA, USA, 1992. IEEE Computer Society Press.